X-ray diffraction analysis of the structure of antisite arsenic point defects in low-temperature-grown GaAs layer

S. Fukushima and N. Otsuka[a)]
School of Materials Science, Japan Advanced Institute of Science and Technology, Asahidai 1-1, Nomishi, Ishikawa 923-1292, Japan

(Received 14 November 2006; accepted 26 January 2007; published online 9 April 2007)

A method for the structure analysis of point defects in a semiconductor layer is developed by combining x-ray diffraction and growth of a superlattice where the concentration of point defects is periodically varied in the growth direction. Intensities of satellite reflections from the superlattice depend predominantly on the atomic structure of point defects, and hence this method can be applicable to the case of a low concentration of point defects. By using this method, the atomic structure of antisite As point defects in GaAs layers grown by molecular-beam epitaxy at low temperatures has been analyzed. Measured intensity ratios of the first-order satellite reflection in the lower angle side to that in the higher angle side for a number of (*hkl*) reflections are compared with those calculated based on structure models. The analysis has shown that experimental intensity ratios cannot be reproduced by models which include only a uniform tetragonal lattice distortion and local atomic displacements around an antisite As atom. A fairly good agreement between measured and calculated intensity ratios is obtained with a model which account for both gradual change in the tetragonal lattice distortion in the (0 0 1) plane and displacements of neighboring atoms away from the antisite As atom. © *2007 American Institute of Physics*. [DOI: 10.1063/1.2715523]

I. INTRODUCTION

Point defects are known to significantly affect electrical and optical properties of semiconductors.[1] Electronic structures and atomic structures of point defects in semiconductors, hence, have been extensively studied in the past mainly by means of spectroscopic methods such as photoluminescence spectroscopy and electron paramagnetic resonance. In recent years first-principles molecular dynamics calculations have been widely used for studies of point defects.

The intensity analysis of x-ray diffraction is the most standard method for analyzing atomic structures of crystalline materials because of its firm theoretical foundation. This method, however, has scarcely been applied to the analysis of atomic structures of point defects in semiconductors because the contribution of point defects to x-ray diffraction intensities is, in general, too small to be used for the analysis.

In this paper we present a method of the x-ray diffraction analysis of point defects in semiconductors. The method combines x-ray diffraction and growth of a superlattice where the concentration of point defects is periodically varied in the growth direction. Satellite reflections from the superlattice result from the periodic variation of the concentration of point defects, and hence their intensities are predominantly determined by the atomic structure of point defects. One can, therefore, directly analyze the atomic structure of point defects with these satellite reflections even if the concentration of point defects is low. This paper reports results of the structure analysis of antisite As(As_{Ga}) atoms in GaAs epilayers grown at low temperatures (LT-GaAs) by molecular-beam epitaxy (MBE) as an example of the application of this method. Past studies on LT-GaAs have shown that antisite As atoms are responsible for ultrafast relaxation of photoexcited carriers in this material where ionized antisite As(As_{Ga}^{+}) becomes trap sites of photoexcited electrons[2] and neutral antisite As(As_{Ga}) becomes main trap sites of photoexcited holes.[3]

The structure of an As_{Ga} point defect in LT-GaAs was experimentally studied first by the ion channeling method.[4] The results of this study were earlier explained by assuming the existence of interstitial As point defects, but later the same results were explained with As_{Ga} point defects associated with displacements of neighboring atoms.[5] Liu *et al.* have reported a linear relationship between the tetragonal distortion of the LT-GaAs lattice and the As_{Ga} concentration which was estimated by using near-infrared absorption.[5] This linear relationship suggests that the majority of excess As point defects in LT-GaAs are As_{Ga} atoms. Sano *et al.*[6] reported that the intensity of forbidden Raman scattering of longitudinal and transverse optical phonons in LT-GaAs linearly increased with the As_{Ga} concentration, which implies that As_{Ga} point defects have a symmetry lower than the T_d symmetry.

The atomic structure of an As_{Ga} point defect has been investigated by a number of theoretical studies. Chadi and Chang[7] proposed, on the basis of their *ab initio* total energy calculations, that in an energetically stable As_{Ga} point defect, neighboring atoms moved radially away from the antisite atom by 0.019 nm. In the metastable structure found in their study the As_{Ga} atom moved by 0.12 nm in the [1 1 1] direction from the ideal antisite position. Landman *et al.*[8] used first-principles molecular-dynamics calculations and reported that a low energy As_{Ga} related point defect had a complex structure consisting of an As_{Ga} atom and two As interstitial

[a)]Author to whom correspondence should be addressed; FAX: 81-761-51-1149; electronic mail: ootsuka@jaist.ac.jp

atoms. More recently Staab *et al.*[9] studied lattice distortions caused by excess As point defects by utilizing a self-consistent-charge density-functional based tight-binding method which was capable of treating a large number of atoms. Theoretical values of the tetragonal lattice distortions caused by As_{Ga} atoms agree well with the experimental values of LT-GaAs, while those caused by interstitial As atoms do not, which indicates that the dominant point defects in LT-GaAs are As_{Ga} atoms. In the As_{Ga} atomic structure derived in their study, the nearest neighbor atoms as well as the next nearest neighbor atoms moved away from the As_{Ga} atom by 0.031 and 0.009 nm, respectively.

In an earlier study we have found that the As_{Ga} concentration in LT-GaAs can be changed by changing the As/Ga flux ratio at a constant substrate temperature.[10] By utilizing this method we have grown LT-GaAs superlattice structures in which the As_{Ga} concentration periodically varies in the growth direction. For the analysis the intensity ratios of the first-order satellite reflection in the lower angle side to that in the higher angle side for a number of different (*hkl*) reflections have been compared with those calculated based on selected models. The analysis has shown that experimental intensity ratios cannot be reproduced by models which include only a uniform tetragonal lattice distortion and atomic displacements of the As_{Ga} atom and neighboring atoms. A fairly good agreement between experimental and calculated intensity ratios is obtained with a model, which includes a gradual modulation of the tetragonal lattice distortion in the (0 0 1) plane and displacements of neighboring atoms away from the As_{Ga} atom.

II. EXPERIMENT

A LT-GaAs superlattice structure was grown by using a conventional MBE system. A semi-insulating epiready (0 0 1) GaAs wafer was used as a substrate. After oxide desorption of a substrate surface, a 160-nm-thick GaAs buffer layer was grown at 580 °C. For the growth of a superlattice structure the substrate temperature was lowered to 210 °C which was measured by a pyrometer through a quartz rod installed in the MBE system.[10] The periodic modulation of the excess As concentration was made by using one Ga cell and two As cells with the shutter of one of the As cells being periodically closed and opened. The Ga flux was maintained at a constant ion gauge reading, 5.1×10^{-7} Torr. The flux intensity of one As cell, called As I cell, was set at 6.3×10^{-6} Torr, while the flux intensity of the other As cell, As II cell, was kept at 2.8×10^{-5} Torr. With fluxes of the Ga cell and As I cell a nearly stoichiometric GaAs layer was obtained, while the addition of the flux of the As II cell gave rise to a nearly saturated excess As concentration at this substrate temperature.[10] By setting an identical time length for opening and closing of the shutter of the As II cell, nearly identical thicknesses of two layers with lower and higher excess As concentrations were obtained. Thirty periods were grown with the thickness of individual layers being approximately 22.5 nm which approximately corresponds to a length of 40 GaAs unit cells. The substrate was rotated during the growth in order to obtain a uniform flux condition over the sample surface.

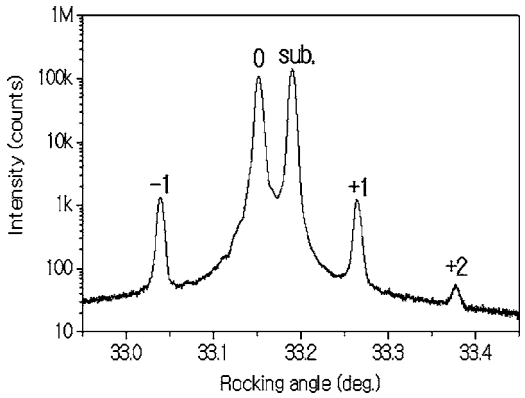

FIG. 1. Rocking curve of the (0 0 4) reflection of a LT-GaAs superlattice sample with its first-order and second-order satellite reflections. In the figure, reflection peaks denoted by 0 and sub. are the (0 0 4) fundamental reflection of the superlattice and the (0 0 4) reflection of the GaAs substrate, respectively.

X-ray diffraction experiments were carried out by using a Philips PW3754 diffractometer with a Ge four-crystal monochromator. The Cu $K\alpha$ radiation was used for measurements. Figure 1 is an x-ray diffraction pattern showing the (0 0 4) fundamental reflection peak and its two first-order satellite reflection peaks and the second-order satellite reflection peak in the higher angle side along with the (0 0 4) reflection peak of a substrate. The average (0 0 4) lattice spacing of the superlattice was determined from the angle of the (0 0 4) fundamental reflection peak with respect to that of the (0 0 4) reflection peak of the GaAs substrate. According to our earlier study,[10] the As_{Ga} concentration and hence tetragonal lattice distortion of a LT-GaAs epilayer are known to saturate at constant values under a high As flux condition for a given growth temperature. The (0 0 4) lattice spacing of layers of the superlattice which were grown under the high As flux condition, layer II, was therefore assigned to that of an epilayer grown under the same As flux condition at 210 °C. The (0 0 4) lattice spacing of the layers grown under the lower As flux condition, layer I, was then derived from the average (0 0 4) lattice spacing and that of layer II. The As_{Ga} concentrations in layers I and II were estimated by using the experimental relation between the As_{Ga} concentration, $[As_{Ga}]$ (cm^{-3}), and the tetragonal lattice distortion[5]

$$[As_{Ga}] = \frac{(\Delta d/d)_{004}}{1.24\times10^{23}}. \quad (1)$$

In Table I, As fluxes, (0 0 4) lattice spacings, and As_{Ga} concentrations of two constituent layers of the superlattice are

TABLE I. Arsenic fluxes, (004) lattice spacings, and As_{Ga} concentrations of layers I and II.

Layer	Arsenic flux (Torr)	d_{004} (nm)	$[As_{Ga}]$ (cm^{-3})
I	6.3×10^{-6}	0.141 44	5.84×10^{19}
II	3.43×10^{-5}	0.141 55	1.14×10^{20}

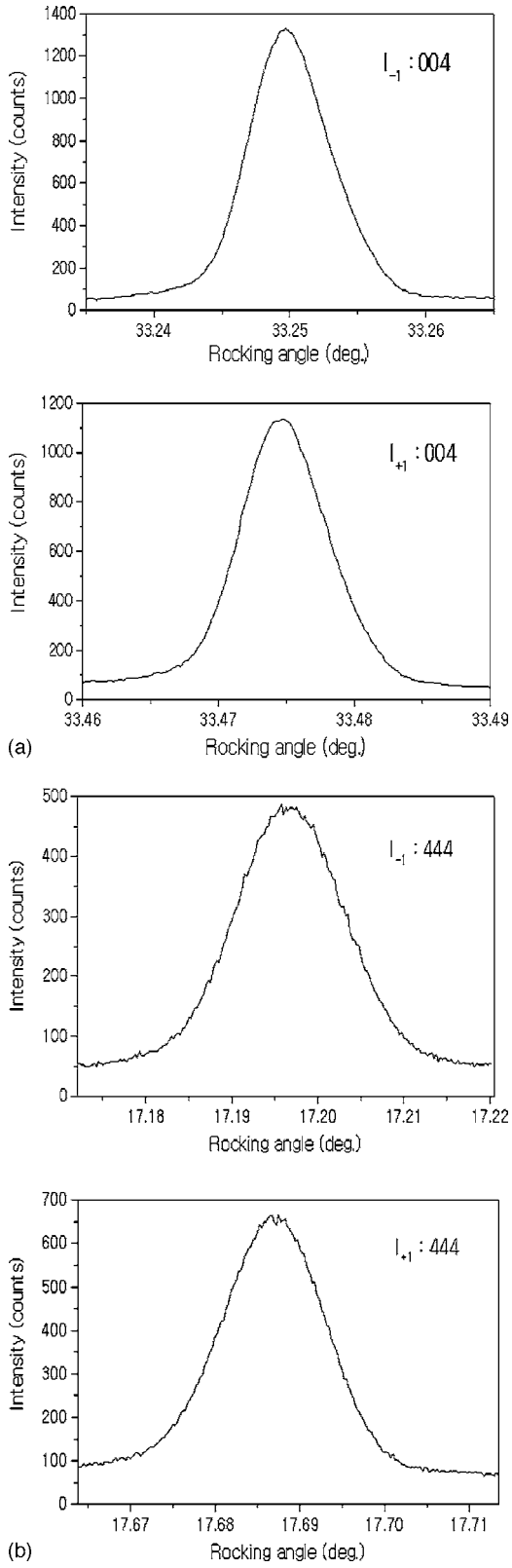

FIG. 2. Rocking curves of first-order satellite reflections for intensity measurements: (a) (0 0 4) reflection and (b) (4 4 4) reflection. In the figure, I_{-1} and I_{+1} indicate first-order satellite reflection peaks in the lower angle side and in the higher angle side, respectively.

listed, which were used for the construction of models as described in the next section.

In the present study, integral intensities of the first-order satellite reflections of the symmetrical reflection (0 0 4) and four asymmetrical reflections (2 2 4), (1 1 5), (3 3 5), and (4 4 4) were measured. These reflections are located in the measurable range of the diffractometer used in the present study. Intensities of satellite reflections of the (0 0 2) reflections are too weak to be used for the accurate quantitative analysis. The intensity ratios of the first-order satellite reflection in the lower angle side to that in the higher angle side, I_{-1}/I_{+1}, for each (hkl) reflection were used for the analysis, the reason for which is explained in Sec. III. For each of the four asymmetrical reflections, the first-order satellite reflections of a pair of reflections, $(h\bar{k}l)$ and $(\bar{h}kl)$, were used. Although higher-order satellite reflection peaks were observed, their intensities were too weak to be used for quantitative analysis and, hence, were not used in the present study.

In order to obtain an accurate intensity ratio of the first-order satellite reflections, rocking curves of the first-order satellite reflections in the lower angle side and higher angle side for a given reflection were slowly scanned alternately four times. Figures 2(a) and 2(b) are examples of rocking curves of first-order satellite reflections of the (0 0 4) and (4 4 4) reflections in both lower and higher angle sides, respectively, which were obtained by this slow scanning. Integral intensities were obtained from rocking curves and were averaged over four measurements. The intensity ratio was then obtained from the average integral intensities of the two first-order satellite reflections. In the case of Fig. 2(a), the intensity ratio of satellite reflections is greater than unity, while in the case of Fig. 2(b), the ratio is smaller than unity.

III. METHOD OF INTENSITY CALCULATION

As a structure model for the intensity calculation, we have constructed a superlattice structure with sizes in the [1 0 0] and [0 1 0] lateral directions being 15 GaAs unit cells and a size in the [0 0 1] growth direction being 30 periods of supercells, each of which consists of two layers, layers I and II. Both layers I and II have thicknesses of 40 GaAs unit cells, where the former has a lower concentration of As_{Ga} atoms and the latter a higher concentration of As_{Ga} atoms. Figure 3 illustrates the configuration of the model of the superlattice structure. The size of 15 GaAs unit cells in the [1 0 0] and [0 1 0] directions was chosen by confirming that this size was large enough to give rise to size-independent intensity ratios of satellite reflections, for which intensity calculations were made by changing the size up to 40 GaAs unit cells in the [1 0 0] and [0 1 0] directions. In layers I and II, As_{Ga} atoms are randomly placed on Ga sites, while the concentration in each layer is made to coincide with experimental values.

On the basis of a given structure model, scattering factors $F(k_x,k_y,k_z)$ of the entire system with 15 GaAs unit cells in both [1 0 0] and [0 1 0] directions and 30 periods of supercells in the [0 0 1] direction are calculated, where k_x, k_y, and k_z are x, y, and z components of a scattering vector, respectively. With these scattering factors, intensities of satellite reflections are calculated by using the equation[11]

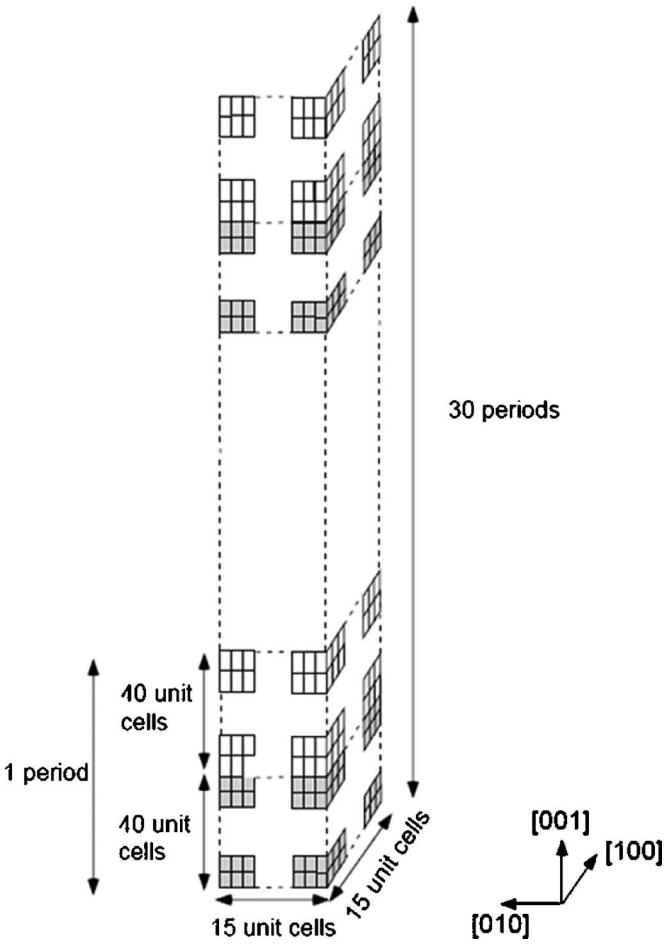

FIG. 3. Structure of a superlattice model for intensity calculations.

$$I(k_x,k_y,k_z) = C|F(k_x,k_y,k_z)|^2 A(\theta)\frac{(1+\cos^2 2\theta)}{\sin 2\theta} \times \exp\left(\frac{-2B\sin^2\theta}{\lambda^2}\right)(1 \mp \cot\theta\tan\varphi), \quad (2)$$

where C is a constant, and θ is the diffraction angle from the sample. Here a lattice plane is inclined to the (0 0 1) sample surface at an angle φ. The signs in front of cot θ depend on whether the angle of incidence is $(\theta-\varphi)$ or $(\theta+\varphi)$. The parameter $B=0.006$ nm^2 in the temperature factor is used.[12] The absorption factor $A(\theta)$ whose formulas for symmetrical and asymmetrical lattice planes are given in Ref. 13 is calculated by using a linear absorption coefficient obtained with atomic absorption coefficients of Ga and As.[14]

In the above calculation, approximate values based on bulk GaAs crystals are used for the absorption coefficient and the parameter B. If one compares intensities of reflections whose diffraction angles are significantly different from one another, effects of these approximations cannot be ignored. From the first-order satellite reflection in the lower angle side to that in the higher angle side for a given (hkl) reflection, however, both absorption factor and temperature factor change by very small fractions being less than 1% because of their close diffraction angles. Similarly other angle-dependent factors in Eq. (3) except for $F(k_x,k_y,k_z)$ change their values by small fractions being less than 1% from the first-order satellite reflection in the lower angle side to that in the higher angle side for a given reflection. The intensity ratio of the first-order satellite reflections I_{-1}/I_{+1} is, hence, predominantly dependent on $F(k_x,k_y,k_z)$ which are, on the other hand, directly determined by structural modulations caused by As_{Ga} atoms. The dynamical diffraction effect on the satellite intensities was estimated by using the two-wave dynamical diffraction theory.[15] For a given model and given satellite reflection, the difference between the intensities based on the dynamical diffraction theory and kinematical diffraction theory is less than 0.2%. The intensity ratios I_{-1}/I_{+1} calculated by using Eq. (1) without including the dynamical diffraction effect were, therefore, used in the present analysis.

TABLE II. Experimental and calculated intensity ratios of first-order satellite reflections.

hkl	$\sin\theta/\lambda$ (nm^{-1})	Expt.	B	C	D_1	D_2
(004)	7.068	1.068(0.005)	0.988	0.959	1.087	1.041
(224)	8.659	0.864(0.007)	1.004	0.956	1.069	0.962
(115)	9.182	0.966(0.005)	0.983	0.937	1.112	0.996
(335)	11.592	0.875(0.006)	1.010	0.939	1.087	0.905
(444)	12.250	0.853(0.004)	1.003	0.930	1.070	0.841

IV. RESULTS OF ANALYSIS AND DISCUSSION

A. Experimental intensity ratios of the first-order satellite reflections

Table II lists experimental intensity ratios of the first-order satellite reflections I_{-1}/I_{+1} for five (hkl) reflections in column Expt. The listed values are averaged ones obtained by repeated measurements of intensities of satellite reflections in the procedure described in Sec. II, and those in parentheses are standard deviations of these averaged values. For each asymmetrical reflection, the average intensity ratio of the $(h\bar{k}l)$ and $(\bar{h}kl)$ reflections is listed. The table shows that the intensity ratio for the 0 0 4 reflection is greater than unity, while those for all other reflections are smaller than unity.

B. Model with idealized As_{Ga} atoms and uniform tetragonal lattice distortion

At the first step of the analysis, we have constructed a model where no local atomic displacement occurs around each As_{Ga} atom and a tetragonal lattice distortion occurs uniformly in each of layers I and II. Because the atomic scattering factor of As is very close to that of Ga, this model is considered as a nearly ideal phase modulation. In the case of the ideal phase modulation where only a lattice spacing is periodically modulated in one direction, intensity ratios of the first-order satellite reflections I_{-1}/I_{+1} are known to be exactly unity for all (hkl) reflections,[16] if one ignores the dependence of the temperature, absorption, Lorentz polarization, and atomic scattering factors on the diffraction angle. In column B of Table II calculated intensity ratios based on this model are listed. The results show that all calculated intensity ratios are close to unity with their deviations being less

than 2% as expected from the above explanation. The observed intensity ratios, on the other hand, deviate from unity by significantly large fractions, which suggests the occurrence of local atomic displacements in the neighborhood of each As_{Ga} atom.

C. Model with local atomic displacements and uniform tetragonal lattice distortion

As explained in the Introduction, Staab *et al.*[9] derived a stable As_{Ga} structure in their recent theoretical study. In the structure the nearest neighbor As atoms and second nearest neighbor Ga atoms are displaced radially away from the As_{Ga} atom by 0.031 and 0.009 nm, respectively, along with a uniform tetragonal lattice distortion whose magnitude is proportional to the As_{Ga} concentration similar to the experimental result.[5] We have calculated intensity ratios of satellite reflections on the basis of this model, and the results are listed in column C of Table II. The results show that the ratios are smaller than unity for all reflections with their deviations ranging from 4% to 7%. According to calculations based on a variety of models, the tendency that intensity ratios are smaller than unity appears to be common for all models which include local atomic displacements and a uniform tetragonal lattice distortion.

The origin of the above-mentioned tendency is explained with a one-dimensionally modulated structure model by following the method given by Takagi.[17] In this model the lattice spacing a_n and structure factor F_n of the nth unit cell change sinusoidally in the [0 0 1] direction with a period L,

$$a_n = a + \Delta a \cos(2\pi na/L), \tag{3a}$$

and

$$F_n = F + \Delta F \cos(2\pi na/L), \tag{3b}$$

where a and F are average lattice spacing and average structure factor, respectively, and Δa and ΔF are amplitudes of their modulation. If $a \ll L$ and $L\Delta al/a^2 \ll 1$, the intensity ratio of the first-order satellite reflections is given by

$$I_{-1}:I_{+1} = \left(\frac{\Delta F}{F} + \frac{L\Delta al}{a^2}\right)^2 : \left(\frac{\Delta F}{F} - \frac{L\Delta al}{a^2}\right)^2. \tag{4}$$

Conditions $a \ll L$ and $L\Delta al/a^2 \ll 1$ are satisfied in the present case. At a higher As_{Ga} concentration Δa increases, but structure factors of reflections resulting from the GaAs zinc-blende-type structure decrease due to local atomic displacements in the neighborhood of As_{Ga} atoms. Signs of Δa and ΔF are, hence, opposite to each other in the case of the LT-GaAs superlattice. This implies that intensity ratio of satellite reflections I_{-1}/I_{+1} of a model which includes local atomic displacements and a one-dimensional modulation of the tetragonal lattice distortion is always smaller than unity. In contradiction to this prediction, the experimental intensity ratio of the (0 0 4) reflection is significantly greater than unity, as seen in Table II.

Next, therefore, we have examined possible origins of the greater-than-unity intensity ratio. LT-GaAs layers are known to contain Ga vacancies in addition to As_{Ga} atoms. According to earlier experimental studies, a concentration of Ga vacancies is only a few percent of that of As_{Ga} atoms.[18] We have calculated intensity ratios of satellite reflections with a model containing Ga vacancies, but the results have shown that the effect of the existence of Ga vacancies on the intensity ratios is negligible because of their very low concentration.

Up to this point abrupt interfaces between layers I and II have been assumed for all models, but interfaces in the real sample are considered to be diffused to a certain extent because of the roughening of the growth front and migration of excess As atoms across the interface. In order to examine the effect of the diffused interface on the intensity ratios, we made two models where interfaces between layers I and II extended over five and ten GaAs unit cells in the [0 0 1] direction, respectively. In these models the As_{Ga} concentration is changed linearly in the interface regions from layers I to layer II. The calculations have shown that intensity ratios of higher-order satellite reflections change significantly with the broadening of interfaces, but the intensity ratios of the first-order satellite reflections are nearly unaffected by the interface broadening; the intensity ratio of the first-order satellite reflections of the (0 0 4) reflection decreases only by 1% and 2% as the interface width increases to five and ten GaAs unit cells, respectively. One cannot, therefore, ascribe the greater-than-unity intensity ratio of the (0 0 4) reflection to the interface broadening.

D. Models with nonuniform tetragonal lattice distortion with local atomic displacements

In the models considered so far, a uniform tetragonal lattice distortion is assumed in each of layers I and II. In a LT-GaAs layer a tetragonal lattice distortion is caused by As_{Ga} atoms under the condition of the pseudomorphic growth on a GaAs substrate. It is, therefore, likely that the magnitude of the tetragonal lattice distortion is largest at the position of an As_{Ga} atom and gradually decreases with an increase in the distance from the As_{Ga} atom. In order to examine the effect of this nonuniform tetragonal lattice distortion on the intensity ratio, we have made the following simplified model.

Figure 4 illustrates a model in which the tetragonal lattice distortion of unit cells gradually decreases in the [1 0 0] direction from an As_{Ga} atom. In the model the [0 0 1] unit cell length of the jth cell is given by

$$a_j = a_0 + \Delta a' + \Delta a''(5 - j) \quad (j = 1 - 4), \tag{5a}$$

and

$$a_j = a_0 + \Delta a' \quad (j \geqslant 5), \tag{5b}$$

where a_0 is the lattice constant of GaAs, $\Delta a'$ a uniform part of the lattice distortion, and $\Delta a''$ a gradient of a nonuniform part of the lattice distortion. The magnitude of the nonuniform part of the lattice distortion is assumed to decrease linearly as j increases from 1 to 4, while the tetragonal lattice distortion is assumed to be uniform in the outside of this region. In the [0 1 0] direction, the nonuniform part of the lattice distortion changes in the similar manner to that in the [100] direction. For a given model, values of $\Delta a'$ and $\Delta a''$ are assigned for each of layers I and II under the condition

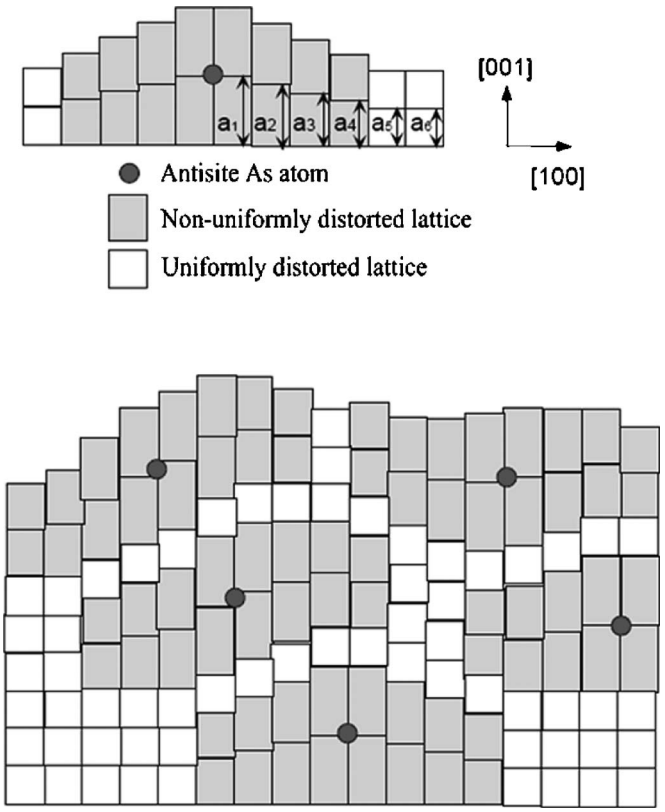

FIG. 4. Model of nonuniform tetragonal lattice distortion.

that the average lattice distortion obeys the experimental relation [Eq. (1)] with the As_{Ga} concentration. If locations of more than one As_{Ga} atoms are close to one another, the nonuniform parts of the lattice distortion are simply added to one another in the overlapped area in order to ensure the above experimental relation.

Intensity ratios of satellite reflections were calculated for the model without including local atomic displacements and are listed in column D_1 of Table II. In this model $\Delta a'$ of layers I and II are 0.21 and 0.40 pm, respectively, and $\Delta a''$ of both layers is 0.08 pm. It is seen from the results that intensity ratios are greater than unity for all reflections. Magnitudes of the deviation from unity are similar for all reflections. For other models with different values of $\Delta a'$ and $\Delta a''$, similar results were obtained, which indicates that the inclusion of a nonuniform tetragonal lattice distortion without local atomic displacements always gives rise to greater-than-unity intensity ratios for all reflections.

Local atomic displacements and nonuniform tetragonal lattice distortion, both of which are likely to occur in a real LT-GaAs crystal, give rise to the deviation of the intensity ratios from unity in opposite directions to each other. Experimental intensity ratios listed in Table II, therefore, are likely to be reproduced by a proper combination of these two structure modulations. We, therefore, made calculations of intensity ratios of the five reflections by assuming a variety of values of local atomic displacements of the first, second and third nearest neighbor atoms and those of the parameters $\Delta a'$ and $\Delta a''$ in Eqs. (5a) and (5b). Calculated intensity ratios are compared with experimental ones for each set of the above-mentioned assumed values by using the following reliable index:

TABLE III. Nonuniform tetragonal lattice distortion and local atomic displacements of model D_2. Layer I: $\Delta a=0.15$ pm, $\Delta a''=0.11$ pm. Layer II: $\Delta a'=0.30$ pm, $\Delta a''=0.11$ pm. 1st n. n. As: first nearest neighbor As atoms. 2nd n. n. Ga I: second nearest neighbor Ga atoms located in the same (001) plane with the As_{Ga} atom. 2nd n. n. Ga II: second nearest neighbor Ga atoms located in the same (010) plane with the As_{Ga} atom. 2nd n. n. Ga III: second nearest neighbor Ga atoms located in the same (100) plane with the As_{Ga} atom. 3rd n. n. As: third nearest neighbor As atoms. Δx, Δy, and Δz are displacements in the [100], [010], [001] directions, respectively, and Δr is the total displacement.

	Number of atoms	Δx (nm)	Δy (nm)	Δz (nm)	Δr (nm)
1st n. n. As	4	0.015	0.015	0.015	0.026
2nd n. n. Ga I	4	0.019	0.019	0	0.027
2nd n. n. Ga II	4	0	0.019	0.015	0.024
2nd n. n. Ga III	4	0	0.019	0.015	0.024
3nd n. n. As	8	0.007	0.007	0.005	0.010

$$R = \frac{\sum_{hkl} |(I_{-1}/I_{+1})^{\text{expt}}_{hkl} - (I_{-1}/I_{+1})^{\text{calc}}_{hkl}|}{\sum_{hkl} (I_{-1}/I_{+1})^{\text{expt}}_{hkl}}, \quad (6)$$

where $(I_{-1}/I_{+1})^{\text{expt}}_{hkl}$ and $(I_{-1}/I_{+1})^{\text{calc}}_{hkl}$ are experimental and calculated intensity ratios of hkl reflection, respectively. Table III lists values of local atomic displacements, $\Delta a'$ and $\Delta a''$ of the model which give rise to the smallest reliable index $R=0.0426$ among those of all assumed models. In column D_2 of Table II, intensity ratios calculated based on this model are listed. In this model, the first nearest neighbor atoms are displaced in the radial directions, while displacements of second and third nearest neighbor atoms are slightly inclined to the (001) plane from the radial directions. Magnitudes of displacements of the first and second nearest neighbor atoms are nearly equal to one another, while those of the third nearest neighbor atoms approximately 40% of the former. Magnitudes of these atomic displacements are comparable to those derived in earlier theoretical studies,[7,9] although relative magnitudes of displacements of the first and second nearest neighbor atoms are considerably different from those of the latter. The model described by Table III gives rise to close agreement between calculated and experimental intensity ratios, but it needs to be pointed out that the derivation of this model is based on a few assumptions. First, nonuniform tetragonal lattice distortion is assumed to have a form shown in Fig. 4. Second, local atomic displacements are assumed to occur up to the third nearest neighbor atoms. Finally, all excess As atoms are assumed to be randomly distributed as isolated As_{Ga} atoms.

V. SUMMARY

In the present x-ray diffraction analysis, intensity ratios of first-order satellite reflections have been used in order to minimize effects of the uncertainty of parameters such as the temperature factor and absorption factor of LT-GaAs on the quantitative analysis. Because of the limited number of the data, atomic structures relevant to an As_{Ga} point defect could not be completely determined. For example, the model described by Table III which gives rise to the best agreement

between calculated and experimental intensity ratios was derived by using a few assumptions as explained at the end of the previous section. In spite of such limitation, a few conclusions can nevertheless be drawn from the present analysis. Firstly, the nonunity intensity ratios of first-order satellite reflections provide direct evidence for the significant deviation of the atomic structure of As_{Ga} from the idealized antisite As atom structure. Secondly, the intensity ratio greater than unity in the case of the (0 0 4) reflection indicates a nonuniformity of the tetragonal lattice distortion in each superlattice layer. Thirdly, the overall trend of observed intensity ratios with respect to (*hkl*) reflections can be reproduced by a proper combination of a nonuniform tetragonal lattice distortion and displacements of neighboring atoms away from an As_{Ga} atom.

Finally, the present analysis suggests that the method of combining x-ray diffraction and growth of a superlattice structure can be used for structure analyses of other point defects including solute atoms in a dilute solid solution. The important requirement for its application is the feasibility of the growth of a periodic structure where the concentration of point defects is varied in a controlled manner. In the present analysis of As_{Ga}, intensity ratios of first-order satellite reflections have been used, but other types of intensity data can also be used for the analysis. For example, intensities of satellite reflections relative to those of fundamental reflections or relative intensities of satellite reflections of the different orders can be used in order to derive detailed information of the structure of point defects.

[1] M. Lanno and J. Bourgoin, *Point Defects in Semiconductors I* (Springer-Verlag, Berlin, 1981), Vol. I; *ibid.* (Springer-Verlag, Berlin, 1983), Vol. II.
[2] U. Siegner, R. Fluck, G. Zhang, and U. Keller, Appl. Phys. Lett. **69**, 2566 (1996).
[3] R. Admacicius, A. Krotkus, K. Bertulis, V. Sirutkatis, R. Butkus, and A. Piskarskas, Appl. Phys. Lett. **83**, 5304 (2003).
[4] K. M. Yu, M. Kaminska, and Z. Liliental-Weber, J. Appl. Phys. **72**, 2850 (1992).
[5] X. Liu, A. Prasad, J. Nishino, E. R. Weber, Z. Liliental-Weber, and W. Walukiewicz, Appl. Phys. Lett. **67**, 279 (1995).
[6] H. Sano, A. Suda, T. Hatanaka, G. Mizutani, and N. Otsuka, J. Appl. Phys. **88**, 3948 (2000).
[7] D. J. Chadi and K. J. Chang, Phys. Rev. Lett. **60**, 2187 (1988).
[8] J. I. Landman, C. G. Morgan, and J. T. Schick, Phys. Rev. Lett. **74**, 4007 (1995).
[9] T. E. M. Staab, R. M. Nieminen, J. Gebaur, R. Krause-Rehberg, M. Luysberg, H. Haugk, and Th. Frauenheim, Phys. Rev. Lett. **87**, 045504 (2001).
[10] A. Suda and N. Otsuka, Appl. Phys. Lett. **73**, 1529 (1998).
[11] *International Tables for Crystallography*, edited by A. J. C. Wilson (Kluwer Academic, London, 1995), Vol. C, p. 518.
[12] R. M. Fleming, D. B. McWhan, A. C. Gossard, W. Wiegmann, and R. A. Logan, J. Appl. Phys. **51**, 357 (1980).
[13] *International Tables for Crystallography*, edited by A. J. C. Wilson (Kluwer Academic, London, 1995), Vol. C, p. 521.
[14] *International Tables for Crystallography*, edited by A. J. C. Wilson (Kluwer Academic, London, 1995), Vol. C, p. 189.
[15] R. W. James, *Solid State Physics*, edited by F. Seitz and D. Turnbull (Academic, New York, 1963), Vol. 15, p. 55.
[16] V. Daniel and H. Lipson, Proc. R. Soc. London, Ser. A **181**, 368 (1943).
[17] S. Takagi, *X-sen Kesshougaku II*, edited by I. Nitta (Maruzen, Tokyo, 1961), p. 648.
[18] M. Luysberg, H. Sohn, A. Prasad, P. Specht, Z. Liliental-Weber, E. R. Weber, J. Gebaur, and R. Krause-Rehberg, J. Appl. Phys. **83**, 561 (1998).